

# Extraordinarily Long-Ranged Structural Relaxation in Defective Achiral Carbon Nanotubes

Michael R. C. Hunt\* and Stewart J. Clark

Centre for Materials Physics, Department of Physics, Durham University, South Road, Durham DH1 3LE, United Kingdom  
(Received 18 April 2012; published 26 December 2012)

We present a systematic *ab initio* density functional theory–based study which demonstrates that even one of the simplest defects in single-wall carbon nanotubes, the reconstructed monovacancy (a pentagonal ring and a single dangling bond known as a 5-1db defect), leads to extraordinarily long-ranged structural distortions. We show that relaxation due to reconstruction can only be modeled accurately through a careful selection of boundary conditions and an appropriately long nanotube fragment.

DOI: [10.1103/PhysRevLett.109.265502](https://doi.org/10.1103/PhysRevLett.109.265502)

PACS numbers: 61.48.De, 61.72.J–, 71.15.Dx

The presence of defects in any real material is an inevitable result of thermodynamics and can impact a range of physical and chemical behaviors. In quasi-one-dimensional materials such as carbon nanotubes the presence of even a low defect density can profoundly alter electronic [1], mechanical [2,3], thermal [4], and chemical [5] properties. A wide range of defects can be formed in carbon nanotubes, discussed in detail in several recent reviews [6–8]. The simplest point defect in single-wall carbon nanotubes (SWCNTs) is the monovacancy, the most common defect resulting from energetic particle irradiation above the atomic displacement threshold [9]. A monovacancy results from removal of a single carbon atom leaving three dangling bonds in an unstable structure which reconstructs, with a small barrier ( $\approx 0.3$  eV in a (3,3) SWCNT [10]), to form a pentagonal ring and a single dangling bond, known as a 5-1db defect [11] (see Fig. 1). The presence of a single monovacancy can lead to profound changes in transport and such defects have been shown to mediate chemical functionalization [12] and catalytic behavior [5]. Therefore, an accurate determination of the structural, electronic, and energetic properties of defects is essential for technological applications of these nanostructures. The defect formation energy is the key parameter since it determines the ease with which defects may arise in nanotubes during growth and subsequent treatment.

The formation energy of isolated 5-1db defects in achiral (armchair and zigzag) SWCNTs has been theoretically determined by a number of researchers [13–18] in calculations employing periodic boundary conditions with super-cells up to 10 unit cells long. Such approaches simulate an infinitely long tube with periodically repeating defects that introduce unphysical defect-defect interactions. Furthermore, this boundary condition cannot model important features such as twisting and bending of the tube. We find that such modes of relaxation are absolutely necessary to accurately model reconstructed vacancies in SWCNTs. Moreover, even with open boundary conditions exceptionally large supercells are required for full relaxation and accurate determination of the defect formation energy, demonstrating the extraordinarily long-ranged

structural distortion associated with the formation of even the simplest vacancy structure in a SWCNT. Our results imply that calculated values for the energies (and hence the derived properties) of reconstructed monovacancies in the literature [13–18] are in error and that the reported formation energies of a wide spectrum of other defects in nanoscale carbon systems need further evaluation.

To determine accurate formation energies for defects and the errors arising from the limited supercell size and the use of periodic boundary conditions we have performed *ab initio* calculations within the density functional, plane-wave, pseudopotential formalisms. The GGA PBE functional is chosen [19], although trends reported are identical for the non-gradient-corrected LDA functional (see the Supplemental Material [20]). We adopt this approach over quantum chemical or linear scaling methods since the latter use localized basis sets and, given the large number of atoms in the work presented here, such basis sets would need to be small and hence the accuracy of the bonding configurations of the defects might be questionable. Plane wave basis sets are known for completeness and hence good accuracy and are thus our basis set of choice. The CASTEP code [21,22] has been used throughout. Spin-polarized electronic wave functions are expanded in a plane wave basis set with an energy cutoff of 380 eV

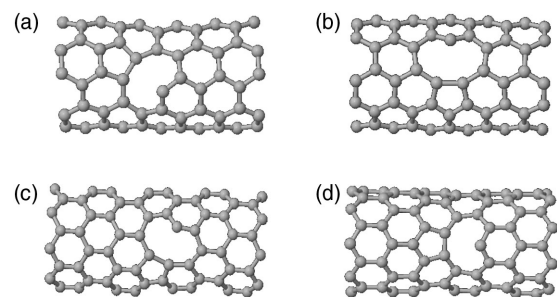


FIG. 1. (a) An *a*-tilt 5-1db defect in a (5,5) nanotube; (b) an *a*-circ defect in a (5,5) nanotube; (c) the *z*-tilt defect in a (9,0) nanotube; (d) a *z*-axial defect in a (9,0) nanotube. For clarity only the topmost atoms close to the defect are shown.

and CASTEP's standard carbon and hydrogen ultrasoft pseudopotentials, built using the mechanisms of Vanderbilt [23], were used to describe the valence-core electron interactions. Our cells are large enough to permit use of a single  $k$  point ( $\Gamma$ ) to sample the Brillouin zone. All calculations were performed in a supercell with a vacuum gap of at least 10 Å between tubes in all directions, which eliminates intertube interactions. The electronic structure was relaxed using a density mixing algorithm and considered converged when energy differences changed less than  $1.0 \times 10^{-6}$  eV/atom. Structural relaxation was performed with a Broyden-Fletcher-Goldfarb-Shanno algorithm using the *ab initio* forces. The structure was considered relaxed when the maximum residual force on any atom was less than 0.01 eV/Å. These controllable convergence criteria ensure that defect energies quoted are accurate to better than 0.05 eV. Additionally, the structural relaxation was performed from several starting configurations to investigate the possibility of local structural minima. We found the same relaxed structure in all test cases irrespective of starting configuration. We also considered spin-polarization of the ends of the zigzag nanotubes. We performed calculations with the ends being 'ferromagnetically' and 'antiferromagnetically' coupled. The energy differences between each pair of states rapidly decreases with length and is less than 0.05 eV/nanotube even for the shortest (4 unit cell) nanotubes considered. The lower energy results are presented in this Letter.

Formation energies have been determined for 5-1 db defects in (i) periodic (5,5) armchair SWCNTs for supercells up to 50 unit cells long (corresponding to 1000 atoms) and (ii) isolated, hydrogen-terminated, fragments up to the same size. We present results of similar calculations on (9,0) zigzag SWCNTs, chosen since they have a similar diameter to (5,5) nanotubes (the diameters are 6.78 and 7.05 Å, respectively), on system sizes up to 25 unit cells (900 atoms) by which size the calculations using free boundary conditions are found to be well converged. All 5-1 db defects were found to be spin polarized, as were the ends of the zigzag nanotubes. We consider both possible orientations of the 5-1db defect with respect to the nanotube axis. In the (5,5) armchair nanotube we label these  $a$ -tilt [see Fig. 1(a)] and  $a$ -circ [see Fig. 1(b)] defects. We also consider 5-1db defects in isolated zigzag (9,0) SWCNTs, which we label  $z$ -tilt [see Fig. 1(c)] and  $z$ -axial [see Fig. 1(d)] defects. We find that the behavior of defect energies with respect to length is qualitatively different between zigzag and armchair SWCNTs indicating the importance of the chiral vector in structural relaxation. We expect that the behavior of chiral nanotubes will be intermediate between that of zigzag and armchair SWCNTs and focus on achiral species due to the large unit cells in chiral nanotubes.

We define the formation energy of a monovacancy,  $\Delta^n$ , of a nanotube of length (or periodicity)  $n$  unit cells, as the

difference in total energy of a fully relaxed nanotube with a single reconstructed vacancy and a structurally relaxed perfect tube of the same supercell length less the energy of a perfect single atom; thus

$$\Delta^n = E_d(n) - \left[ E_p(n) - \frac{1}{n_{\text{cell}}} [E_p(n) - E_p(n-1)] \right], \quad (1)$$

where,  $E_d(n)$  is the energy of a nanotube with a reconstructed monovacancy,  $E_p(n)$  is the energy of a perfect nanotube, and  $n_{\text{cell}}$  is the number of atoms per unit cell. In Fig. 2(a) we show the formation energy of an  $a$ -tilt monovacancy located at the center of an isolated hydrogen-terminated (5,5) SWCNT as a function of nanotube length. The defect formation energy has an extraordinarily long decay with respect to length. This feature has not been observed before and casts doubt upon previously reported results of defect properties obtained by similar *ab initio* methods. We have modeled the data using functional forms that can give a more detailed physical interpretation to the relaxation mechanism. We find the most satisfactory fit is obtained with

$$\Delta^n = \Delta^\infty - A \exp\left(-\frac{l}{a}\right) + B \exp\left(-\frac{l}{b}\right), \quad (2)$$

where  $l$  is the length of the nanotube,  $a$  and  $b$  are decay lengths,  $A$  and  $B$  are constants, and  $\Delta^\infty$  is the formation energy of an isolated 5-1db defect in the limit of an infinitely long nanotube (i.e., fully converged with respect to length). Such a fit yields a formation energy  $\Delta^\infty$  of  $5.0 \pm 0.3$  eV for an isolated 5-1db defect. This result is compared with formation energies from the literature in Table I. The first exponential term in the fit decays rapidly with length, while the second is very long-ranged.

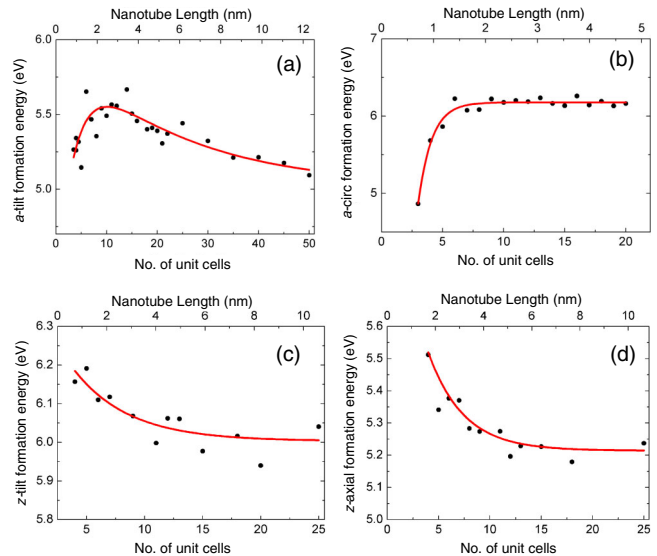


FIG. 2 (color online). Monovacancy formation energies for the (a)  $a$ -tilt defect, (b)  $a$ -circ defect, (c)  $z$ -tilt defect, and (d)  $z$ -axial defect. The lines are fits using the functions described in the text.

TABLE I. Reconstructed monovacancy formation energies in (5,5) and (9,0) SWCNTs (in electron volts). ‘Free’ refers to fully converged calculations and ‘PBC’ to average values obtained from calculations with periodic boundary conditions.

Defect	Free	PBC	Reference [13]	Reference [14]	Reference [16]	Reference [17]
<i>a</i> -tilt	$5.0 \pm 0.3$	5.7	5.6	5.05	5.8	5.75
<i>a</i> -circ	$6.2 \pm 0.1$	6.7	7.1	Unstable		
<i>z</i> -axial	$5.2 \pm 0.1$		5.4	4.7	5.4	6.7
<i>z</i> -tilt	$6.0 \pm 0.1$		6.4	6.0		

A similar variation in the monovacancy formation energy to that seen in the shortest tubes (i.e., those with a 5-1 db formation energy dominated by the first exponential term) was found for defects near nanotube ends by Ding [24] but in that study the geometry of the reconstruction differed with the distance of the defect from the nanotube end.

Our calculations show that the lower defect formation energy for short armchair SWCNTs arises from asymmetric radial distortion along the whole nanotube length (see the Supplemental Material [20]). The second exponential term is significant, but the use of limited length and periodic boundary conditions in earlier work quenched this important degree of freedom. It has an extremely long decay length and demonstrates the presence of a previously unobserved, long-ranged component to the strain associated with defect reconstruction. This long-ranged strain originates from a ‘twist’ about the reconstructed monovacancy which decays in amplitude with distance (see Fig. 3). Since previous *ab initio* studies employing periodic boundary conditions could not take this relaxation mode into account they substantially overestimate the defect formation energy (see Table I). The *a*-tilt formation energy determined in the approximate tight-binding calculations of Lu and Pan [14] appear to be in closer agreement with our results than *ab initio* studies [13,15–18]. However, this

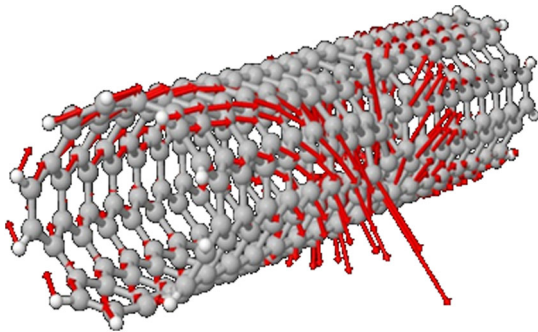


FIG. 3 (color online). Relaxation of an 18 unit cell (5,5) nanotube due to a monovacancy. Arrows show the direction in which atoms move from their original positions due to reconstruction. The relative length of the arrow corresponds to relative displacement of the atom and is not to scale. A video showing the displacement of the atoms is provided in the Supplemental Material [20].

is the result of an underestimated formation energy canceling uncompensated strain energy arising from the application of periodic boundary conditions and a small supercell: Lu and Pan use the same combination of supercell size and periodic boundary conditions as in the *ab initio* calculations of Wang and Wang [16] for both *a*-tilt and *z*-axial defects and in both find the formation energy  $\approx 0.7$  eV lower. Moreover, Lu and Pan themselves point out that they find the formation energy of the monovacancy defect in graphene  $\approx 0.6$  eV smaller than that found by *ab initio* approaches [14].

With free boundary conditions we find that a length of 55 unit cells (1100 carbon atoms) is required to converge the defect formation energy to within (a still significant) 0.1 eV. However, when applying periodic boundary conditions there are no circumstances in which the energy can be converged with length since the full range of structural relaxation cannot be considered. Indeed, we find that with periodic boundary conditions the vacancy formation energies fluctuate over  $\approx 2$  eV (see the Supplemental Material [20]) as the supercell length changes. The average defect formation energy with periodic boundary conditions (‘PBC’ in Table I) is found to be 5.7 eV (similar to that previously reported [13,15,17]) which is  $0.7 \pm 0.3$  eV above that for the fully relaxed tube. This indicates a large energy cost associated with the incomplete relaxation in previously reported studies.

The *a*-circ defect was previously thought to be unstable [14], undergoing a barrierless transition to an *a*-tilt defect. We find similar results for small ( $\leq 8$  unit cell) supercells with periodic boundary conditions (see the Supplemental Material [20]). However, in larger periodic supercells or for any size nanotube with free boundaries we find that this defect is actually metastable, indicating that (unphysical) interacting strain fields led to the previously observed instability. In Fig. 2(b) we present the formation energy for the *a*-circ defect in (5,5) nanotubes as a function of nanotube length. We model this variation using the function

$$\Delta^n = \Delta^\infty - C \exp\left(-\frac{l}{c}\right), \quad (3)$$

where  $C$  is a constant and  $c$  is the decay length, with other variables as defined in Eq. (2). The fit yields a defect formation energy of  $6.2 \pm 0.1$  eV. The decay length of

this function is the same magnitude as that of the first term in Eq. (1), showing that it is associated with the same asymmetric radial relaxation of the nanotube, which cannot be captured with periodic boundary conditions. Calculations of the *a*-circ formation energy using periodic boundary conditions and supercells up to 22 unit cells (440 atoms) in size also demonstrate no obvious convergence, with an average value of 6.7 eV (compared with 6.2 eV for open boundaries; see Table I).

The long-ranged relaxation mechanisms we observe in the zigzag nanotubes are qualitatively different from those of armchair nanotubes. In the former decay is more rapid, but still longer ranged than typically found for defects in bulk crystalline materials. We show the defect formation energy as a function of nanotube length for *z*-tilt and *z*-axial monovacancies in a (9,0) nanotube in Figs. 2(c) and 2(d). The variation can be fitted by a single function similar to that used for the *a*-circ defect but with a change of sign of the exponential prefactor. Such fitting yields decay lengths of  $5 \pm 2$  and  $3 \pm 1$  unit cells and defect formation energies of  $6.0 \pm 0.1$  eV and  $5.2 \pm 0.1$  eV for the *z*-tilt and *z*-axial defects, respectively. Thus, we find end effects dominate the dependence of the vacancy formation energy with length. The defect energy in shorter carbon nanotubes is larger than that in longer tubes (opposite to that observed in armchair SWCNTs). This difference is a result of the stiffness of the zigzag ends, suppressing the relaxation observed in short armchair nanotubes (see the Supplemental Material [20]). We would expect that capped nanotubes would show greater resistance to deformation than hydrogen terminated nanotubes and thus display a larger defect formation energy at short lengths than in the uncapped cases. For *z*-axial defects, our results are similar to those found by workers employing periodic boundary conditions [13,16,17] (see Table I); the smaller influence of boundary conditions on the defect formation energy in comparison with the (5,5) armchair nanotubes is a result of the ends of the zigzag nanotube retaining an almost unperturbed structure due to their stiffness to displacements which accommodate the structural relaxation associated with reconstruction. The value we find for the formation energy of the isolated *z*-tilt defect,  $6.0 \pm 0.1$  eV, is smaller than the value of 6.4 eV found by Ma *et al.* [13], the difference possibly arising from the longer decay length for this defect.

Our results clearly demonstrate that the structural relaxation associated with reconstruction of an isolated monovacancy defect within a graphitic nanotube lattice can be extraordinarily long ranged (far longer than in any ‘conventional’ solid), most notably for the lowest energy reconstructed monovacancy in armchair nanotubes where, for a (5,5) nanotube the 5-1db formation energy can only be converged to within 0.1 eV for a nanotube fragment 55 unit cells (13.5 nm) long. We also observe similar effects in achiral SWCNTs with different indices [25].

This (chirality dependent) extent of structural distortion arises from a combination of the greater degree of structural freedom offered at the nanoscale in comparison with analogous bulk solids and the unique flexibility associated with bonds in the graphite lattice. Such a relaxation can only be fully captured by calculations on nanotube segments much larger than any *ab initio* calculations on these systems previously considered in the literature. Moreover, periodic boundary conditions cannot capture the nature of these structural defects and the selection of open boundaries is a necessity. The importance of these factors will be general to a wide range of defect and impurity structures in nanotubes and related nanomaterials where significant reconstruction or structural distortion occurs. Preliminary studies show that polyvacancy defects in SWCNTs and both monovacancy and Stone-Wales defects in graphene nanoribbons have a similar need for an appropriate choice of boundary conditions and system size [25]. As a result, it is likely that much published data derived from *ab initio* calculations of defective or functionalized carbon nanostructures to date have treated systems of insufficient size or with unphysical constraints (periodic boundary conditions) and therefore require careful evaluation.

The authors thank the EPSRC for the award of time at the UK National Supercomputing Facility.

---

\*m.r.c.hunt@durham.ac.uk

- [1] C. Gómez-Navarro, P.J. de Pablo, J. Gómez-Herrero, B. Biel, F.J. Garcia-Vidal, A. Rubio, and F. Flores, *Nat. Mater.* **4**, 534 (2005).
- [2] Q. Wang, W.H. Duan, N.L. Richards, and K.M. Liew, *Phys. Rev. B* **75**, 201405 (2007).
- [3] Z.H. Xia, P.R. Guduru, and W.A. Curtin, *Phys. Rev. Lett.* **98**, 245501 (2007).
- [4] J. Wang, L. Li, and J.-S. Wang, *Appl. Phys. Lett.* **99**, 091905 (2011).
- [5] M.K. Kostov, E.E. Santiso, A.M. George, K.E. Gubbins, and M.B. Nardelli, *Phys. Rev. Lett.* **95**, 136105 (2005).
- [6] F. Banhart, *Rep. Prog. Phys.* **62**, 1181 (1999).
- [7] A.V. Krasheninnikov and F. Banhart, *Nat. Mater.* **6**, 723 (2007).
- [8] A.V. Krasheninnikov and K. Nordlund, *J. Appl. Phys.* **107**, 071301 (2010).
- [9] A. Tolvanen, J. Kotakoski, A.V. Krasheninnikov, and K. Nordlund, *Appl. Phys. Lett.* **91**, 173109 (2007).
- [10] Y. Miyamoto, S. Berber, M. Yoon, A. Rubio, and D. Tomanek, *Chem. Phys. Lett.* **392**, 209 (2004).
- [11] P.M. Ajayan, V. Ravikumar, and J.-C. Charlier, *Phys. Rev. Lett.* **81**, 1437 (1998).
- [12] A.J. Lu and B.C. Pan, *Phys. Rev. B* **71**, 165416 (2005).
- [13] Y. Ma, P.O. Lehtinen, A.S. Foster, and R.M. Nieminen, *New J. Phys.* **6**, 68 (2004).
- [14] A.J. Lu and B.C. Pan, *Phys. Rev. Lett.* **92**, 105504 (2004).
- [15] H.Y. He and B.C. Pan, *Phys. Rev. B* **77**, 073410 (2008).
- [16] C. Wang and C.Y. Wang, *Eur. Phys. J. B* **54**, 243 (2006).

- [17] A. V. Krasheninnikov, P. O. Lehtinen, A. S. Foster, and R. M. Nieminen, *Chem. Phys. Lett.* **418**, 132 (2006).
- [18] J. M. Carlsson, *Phys. Status Solidi B* **243**, 3452 (2006).
- [19] J. P. Perdew, K. Burke, and M. Ernzerhof, *Phys. Rev. Lett.* **77**, 3865 (1996).
- [20] See Supplemental Material at <http://link.aps.org/supplemental/10.1103/PhysRevLett.109.265502> for results of calculations employing periodic boundary conditions and of calculations performed using the LDA exchange correlation functional; details of structural relaxation in short nanotubes; a video showing the structural relaxation associated with reconstruction of a monovacancy in an 18 unit cell (5,5) nanotube to form an *a*-tilt defect.
- [21] S. J. Clark, M. D. Segall, C. J. Pickard, P. J. Hasnip, M. I. J. Probert, K. Refson, and M. C. Payne, *Z. Kristallogr.* **220**, 567 (2005).
- [22] M. D. Segall, P. J. D. Lindan, M. J. Probert, C. J. Pickard, P. J. Hasnip, S. J. Clark and M. C. Payne, *J. Phys. Condens. Matter* **14**, 2717 (2002).
- [23] D. Vanderbilt, *Phys. Rev. B* **41**, 7892 (1990).
- [24] F. Ding, *Phys. Rev. B* **72**, 245409 (2005).
- [25] M. R. C. Hunt and S. J. Clark (unpublished).